Litterature Reivew on Lattice QCD Studies of Tetraquarks Candidates $\mathbf{D_{s0}(2317)^{\pm}}$ and $\mathbf{Z_c^{\pm}(3900)}$

2202545

School of Physics & Astronomy, University of Glasgow

Abstract. In the early 2000's, several results were found experimentally in particle collision detectors which did not fit expectations. Many theories were proposed in order to describe these new exotic particles, one of them being that the quark model should be expanded to include more categories of hadrons; tetraquark, pentaquarks, glueballs, etc. This paper presents a literature review on the results from lattice QCD studies on the two tetraquark candidates $D_{s0}(2317)^{\pm}$ and $Z_c^{\pm}(3900)$. Lattice QCD is a numerical method used to simulate particle systems moving through spacetime and can be used for theoretically determining energy levels, and therefore also masses. It was found that the lattice QCD results for $D_{s0}(2317)^{\pm}$ generally agreed with the experimental observations but the structure of the particle is unknown; its mass is slightly low for it being a regular excited state of a $c\bar{s}$ meson. It is hence proposed to be a meson-meson molecule or tetraquark. Studies did not find an energy level corresponding to $Z_c^{\pm}(3900)$ which could be due to the lattice calculations not being precise enough or that the experimental results have a different origin. There can therefore not be drawn a conclusion on the existence of tetraquarks as experimental and theoretical results need to undisputedly agree.

1. Introduction

Physics is continuously trying to confirm or disprove the current understanding of our universe. For this purpose, massive particle collides were build, sending particles hurtling towards each other near the speed of light to collide and hopefully produce unseen particles. Many theoretically predicted particles have been discovered this way, but sometimes the experimental results does not correspond to what theory expects, which is when the hope of new physics kicks in; the hope that there has been found a hole or flaw in our current understanding, that we know is not completely correct. This could be particles with unexpected masses or which have combinations of quantum numbers that do not follow the Standard Model (SM) of particle physics.[1] One of the first examples of this, is the $X(3872)$ which was first observed in early 2003 and aftewards found in many other experiments through several other decays schemes. It's quantum numbers ($J^{PC} = 1^{++}$) did not fit in the quark model and it therefore it sparked the interest for new exotic particles. Since then a number of other particles have been found including the $D_{s0}(2317)^{\pm}$ and $Z_c^{\pm}(3900)$ which are both tetraquark candidates.[2] The particles are all hadrons and should be described by quantum chromodynamics and the quark model which are described in section 2. An overview of the theory of Lattice QCD and the methods used are in section 3 The experimental results for the two particles can be found in section 4 whilst the result of Lattice QCD studies are in 5. In section 6, a comparison of the different lattice QCD studies is carried out together with a general discussion of the future of tetraquarks.

2. Quantum Chromodynamics and The Quark Model

Quantum Chromodynamics (QCD) is the theory of the strong force describing the interaction between particles with colour charge, quarks and gluons. Gluons are massless force carriers with colour charge [3] and quarks are elementary particles with mass, electric charge Q, colour charge, and quantum numbers; spin S, total angular momentum J, parity P [1], and charge parity C [2]. Quarks come in six different flavours; up (u), down (d), charm (c), strange (s), bottom (b) and top (t).[4] Colour charge is an intrinsic property which can take three "values"; red, green and blue (r, g, b). Different combinations of colour charge result in colourlessness such as $r + g + b$, $\bar{r} + \bar{g} + \bar{b}$, $r + \bar{r}$, etc. where $\bar{r}, \bar{g}, \bar{b}$ are anti-colours. Due to the strength of the strong force, gluons and quarks are confined; quarks are only observed in colourless bound states called hadrons. The simplest hadrons are mesons (quark-antiquark) and baryons (three quarks) but other possibilities such as tetraquarks (diquark-antidiquark) and pentaquarks (4 quarks and one aniquark) are also colourless. If one includes gluons in hadrons, one can setup structures suh as glueballs consisting of two or three gluons, or hybrid states consisting of a mixture of quarks and gluons. Empirically only mesons or baryons have been definitely observed as bound and stable hadron states.[1] Hadrons are classified by their quantum numbers but several hadrons can have the same quantum numbers and therefore other properties such as the mass of the hadron must be used in order to uniquely classify them. [5] The quarks that contribute to the hadron's quantum numbers are called *valence quarks* and the quark model describes hadrons using these quarks.[1] Inside the hadrons exist a "soup" of gluons and virtual quark-antiquark pairs, existing due to vacuum energy fluctuations, called *sea quarks*.[6]

QCD is a field theory containing two types of fields; matter fields which are six quark fields, $\psi(x)$, differing only by their corresponding masses (1) and a force field which is a massless gluon field, $A_\mu(x)$, (2). In the equations $\mathbf{r}$ denotes the position vector, t time and f flavour of quark.

$$\psi^{(f)}(x) \equiv \psi^{(f)}(\mathbf{r}, t) \quad f \in \{u, d, s, c, t, b\} \qquad (1) \qquad\qquad A_\mu(x) \equiv A_\mu(\mathbf{r}, t) \qquad (2)$$

The fields contain the properties of their respective particle and systems of particles are excitations of localized energy on the field. In quantum mechanics all particles are described by their wavefunction where the absolute square of it is the probability density of finding the particle at a position, $|\Psi(\mathbf{r})|^2$.[5]

3. Lattice QCD

Lattice QCD is a numerical approximation of QCD using Feynman path integrals and Monte Carlo integration on discretized spacetime on a lattice.[7] No new parameters are needed in the discretisation and it is ab initio, meaning from first principles.[8] It is one of few methods to solve QCD as it is almost impossible to analytically solve using perturbation theory due to the large value of the strong coupling constant, $(\alpha_s \approx 1)$. Only few input parameters are needed in order to tune a lattice QCD simulation; the strong coupling constant and quark masses which are fixed after experimental results of hadron masses. The top quark is not included as a parameter as its lifetime is so short that it is considered not to form bound states.[7] Lattice QCD is used in order to figure out whether QCD is the correct theory for the strong interaction or if another theory should be used instead.[5] This is done through studying decay constants, hadron masses, determining the quark masses and the strong coupling constant.[9]

[1] Parity describes the behavior of a particle's wavefunction when its spatial coordinates are inverted through origin, it can take values + or − referring to even or odd parity.[10]

[2] Charge Parity describes the behavior of a particle's wavefunction when it is transformed into its anti-particle by charge conjugation, it can take values + or − referring to the electric charge sign of the two particles which can be the same or opposite.[11]

3.1. ***Path Integral***

Lattice QCD uses path integrals, namely Feynman path integrals, which are connected to Feynman diagrams and describes the probability of a state going from $\Psi(x_i, t_i)$ to $\Psi(x_f, t_f)$. In order to do this, we need to understand how a state evolves over time. The time-evolution (the *Schrödinger Picture*) of an eigenstate is given by equation (3) where $\hat{U}$ is the time-evolution operator and $\hat{H}$ is the Hamiltonian operator. [12]

$$|\Psi, t\rangle = \hat{U}(t, t_0)\,|\Psi, t_0\rangle \text{ with } \hat{U}(t, t_0) = e^{-\frac{i}{\hbar}(t-t_0)\hat{H}} \tag{3}$$

The transition amplitude or probability amplitude of having eigenstate $|\Psi_f, t_f\rangle$ when making a measurement at time t is equation (4), here Ψ_i represents the eigenstate at time $t = t_0$. It is also known as the *propagator* as it propagates a system through spacetime. [13]

$$\langle \Psi_f, t|\Psi_i, t_0\rangle = \langle \Psi_f, t_0|\hat{U}|\Psi_i, t_0\rangle = \langle \Psi_f, t_0|e^{-\frac{i}{\hbar}(t-t_0)\hat{H}}|\Psi_i, t_0\rangle \tag{4}$$

For lattice QCD, the eigenstates in question are position eigenstates and the equation can therefore be written as $\langle x_f|e^{-\frac{i}{\hbar}(t-t_0)\hat{H}}|x_i\rangle$ for initial and final position eigenstates $|x_i\rangle$ and $|x_f\rangle$. The transition amplitude is equal to the sum over all possible paths as seen in equation (5). Each path is weighted by the classical action, $S[x]$, given by equation (6), where L is the Lagrangian.[14] This path integral and classical action have had time rotated to Euclidean spacetime by $(-it \to t)$ in order to get rid of phases and therefore simply later calculations. [5]

$$\langle x_f|e^{-\hat{H}(t_f-t_i)}|x_i\rangle = \int \mathcal{D}x(t)e^{-S[x]} \tag{5}$$

$$S[x] \equiv \int_{t_i}^{t_f} L(x, \dot{x})dt \equiv \int_{t_i}^{t_f} \left[\frac{m\,\dot{x}(t)^2}{2} + V(x(t))\right] dt \tag{6}$$

Each path, called a *configuration*, in $\int \mathcal{D}x(t)$ is described by a function $x(t)$ and in order to solve the equation, the path integral is simplified by considering time to be discrete and periodic. This is done by defining $t_j = t_i + ja$ for $j = 0, 1, ..., N$ with grid spacing $a \equiv \frac{f_f - t_i}{N}$ and by $T = aN_T \to t_n = t_{n+N_T}$ where N_T is the number of lattice sites. [5] We hence evaluate each path using intermediate steps at time $t = t_j$ which transforms the infinite dimensional integral into an ordinary integral as seen in equation (7), where $x_j = x(t_j)$. The end points are not included in the integral as they are fixed and A is a normalization factor. The discretization of time is also applied to the integral in equation (6) as seen in equation (8). Here the derivative has be transformed into a finite difference. [13]

$$\int \mathcal{D}x(t)e^{-S[x]} \simeq A\int_{-\infty}^{\infty} dx_1 dx_2 ... dx_{N-1}e^{-S[x]} \tag{7}$$

$$S[x] \simeq \sum_{j=0}^{N-1}\left[\frac{m\dot{x}}{2} + V(x_j)\right] = \sum_{j=0}^{N-1}\left[\frac{m}{2a}\left(x_{j+1} - x_j\right)^2 + aV(x_j)\right] \tag{8}$$

The Monte Carlo method is used in order to solve these equations for large N. It can be seen that the paths (configurations) with large $e^{-S[x]}$ will dominate the integral and hence in order to simplify the calculations it is beneficial to generate configurations which are heavily weighted. A set of configurations is called an *ensemble*. [14]

The left-hand side of equation (5) can be re-written using the sum of energy eigenstates of the Hamiltonian, $|E_n\rangle$;

$$\langle x_f|e^{-\hat{H}(t_f-t_i)}|x_i\rangle = \sum_n \langle x_f|E_N\rangle\, e^{-E_n(t_f-t_i)}\, \langle E_n|x_i\rangle \tag{9}$$

In QCD, the position operator is equivalent to quark $\psi(x)$ and gluon $A_\mu(x)$ field operators which are 4-dimensional functions of spacetime [13], and the classical action is the QCD action consisting of a contribution from both quarks and gluons, seen in equation (10). [5]

$$S_{QCD} = S_{quark} + S_{gluon} \tag{10}$$

3.2. ***Calculating hadron masses***

An example of the use of lattice QCD is calculating masses of particles or particle systems. It is, so far, the only reliable way to calculate the masses of quarks as they are confined to hadrons. [15] The masses of hadrons simulated using lattice QCD are found using the *variational method* with a matrix of two-point correlation functions as seen in equation (11) consisting of quark propagators and gauge fields ordered by the paths. [7]

$$C_{ij} = \langle 0|O_i(t)O_j^\dagger(0)|0\rangle = \sum_{n=1}^{\infty} e^{-E_n t}\, \Psi_i^n\, \Psi_j^{n*} \tag{11}$$

Here $\Psi_i^n = (\Psi^n)_i = \langle n|O_i|0\rangle$ are called *overlaps* and their magnitude indicates the excitement the creation operator causes on the energy eigenstate $|n\rangle$. [5] The equality is constructed using equation (9). Each correlation function describes how a system is created at time $t = 0$ by creation/source operator $\mathcal{O}_j^\dagger(0)$, propagates through spacetime, and is annihilated at time t by annihilation/sink operator $\mathcal{O}_i(t)$. The creation operator acts on the QCD vacuum state $|0\rangle$ creating a *trial* state which is a linear superposition of all states with quantum numbers $I(J^P)$. The annihilation operator then acts on the QCD vacuum state annihilating this trial state. [5] The operators for the purpose of studying tetraquarks are meson-meson and 4-quark/tetraquark operators, depicted in figure 1.[16]

An example of a correlation function is a tetraquark being created at time 0 with $\Psi(0)$, propagates through spacetime where it for example decays or splits up into two mesons which are destroyed at time t with $\Phi(t)$ as depicted in the upper right-hand box in figure 1. Here the quark propagators are depicted as the lines connecting the system at time 0 and t.

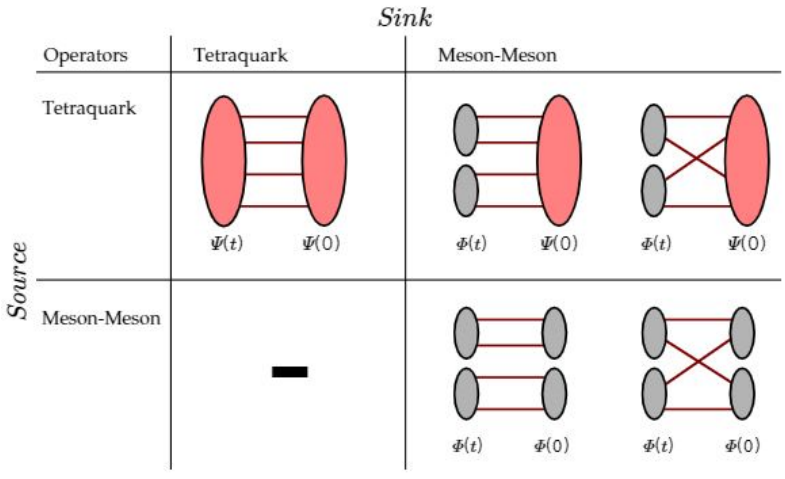

Figure 1: Illustration of different operator setups for computing correlation functions, Ψ denotes tetraquarks, Φ denotes mesons. Picture from [16]

The energy-values of equation (11) are found by solving a generalised eigenvalue problem seen in equation (12) where v_j^n are the eigenvectors and the eigenvalues λ^n the eigenvalues. [16] The eigenvalues $\lambda^n(t,t_0) \propto e^{-E_n t}$ for large values of t and hence the energies/masses of hadrons are extracted. [17]

$$C_{ij}(t)v_j^n = \lambda^n(t,t_0)C_{ij}(t_0)v_j^n \tag{12}$$

3.3. ***QCD on a Lattice***

The lattice used to simulate QCD is set up with spatial and temporal lattice points separated by lattice spacing a and an overall volume L^3T (spatial extent L and temporal extent T). An anisotropic lattice will often be used where the temporal lattice spacing will be different to and smaller than the spatial spacing. Quark fields reside on the sites of the lattice (the lattice points) whilst gluon fields reside on the links connecting the sites as seen on figure 2a.[8] Each site has coordinates $x = (\overrightarrow{x}, t)$ in continuum notation and (x_i, t_i) or $(n_i a, n_t a)$ in lattice notation. As seen on figure 2b, the direction unit vectors $\overrightarrow{\mu}$ and $\overrightarrow{\upsilon}$ are used to define the coordinates of one site with respect to the coordinates of another. Hence the site at x has closest neighbours $x \pm a\overrightarrow{\mu}$ and $x \pm a\overrightarrow{\upsilon}$.

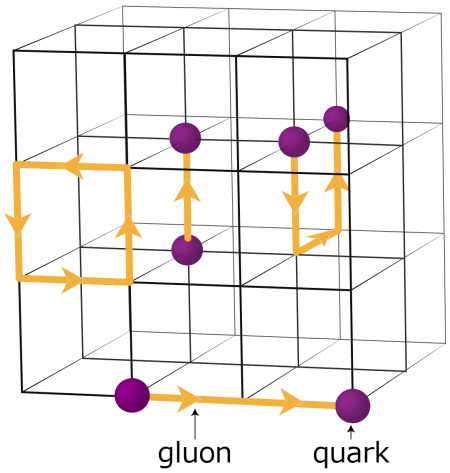

(a) Illustration of discretization of space-time including quark and gluon fields and examples of paths. [18]

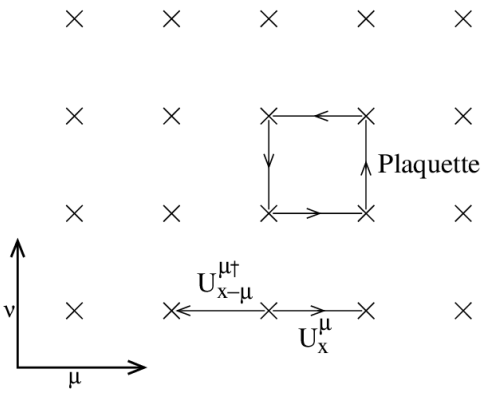

(b) Illustration of a lattice with gluon fields. Image from [19]

Figure 2: Illustrations of the grid-implementation in lattie QCD.

3.4. Gluon Fields

Gluon fields in lattice QCD are 3×3 unitary matrices with determinant $= 1$ defined by equation (13) where A_μ is the continuum gluon field and g the coupling constant of the strong interaction.[5] They are called gauge links and written as either $U_\mu(x)$ or $U_\upsilon(x)$ depending on the direction. x is the lattice point where the link begins and hence the field connecting x and $x + a\overrightarrow{\mu}$ is $U_\mu(x)$ and similarly for $U_\upsilon(x)$ which connects x and $x + a\overrightarrow{\upsilon}$.

$$U_\mu(x) \approx \exp\left(-iagA_\mu\left(x + a\overrightarrow{\mu}\right)\right) \tag{13}$$

$$U_{-\mu}(x + a\overrightarrow{\mu}) = U_\mu^{-1} = U_\mu^\dagger(x) \tag{14}$$

The gluon field connecting the same two sites as $U_\mu(x)$ but with the opposite direction is defined by (14) where $U^\dagger U = 1$.[14]

Paths, gluon fields connecting quarks, and closed loops of gluon fields, like the ones seen on figure 2, are represented by multiplying gluon fields together ordered by the path. The *Wilson Loop function* of a closed path $\mathcal{C}$ is defined by equation(15) and is used to define gauge actions. [20] The example used here is the *plaquette* on figure 2b starting from the lower left-hand corner. This specific Wilson loop is defined as $P_{\mu\upsilon}(x)$.

$$W(\mathcal{C}) = \frac{1}{3}\text{Re Tr}\left(U_\mu(x)U_\upsilon(x + a\overrightarrow{\mu})U^\dagger_\mu(x + a\overrightarrow{\upsilon})U^\dagger_\upsilon(x)\right) \tag{15}$$

The gluonic part of the continuum QCD action, S_{gluon}, is given by (16) where here $F_{\mu\upsilon}$ is the field strength tensor given by equation (17)

$$S_{gluon} = \frac{1}{2}\int d^4x \text{Tr}\left(F_{\mu\upsilon}F^{\mu\upsilon}\right) \tag{16}$$

$$F_{\mu\upsilon} = \delta_\mu A_\upsilon - \delta_\upsilon A_\mu + ig[A_\mu, A_\upsilon] \tag{17}$$

In order to implement this in lattice QCD, different methods can be used in order to discretise this action where some of these are described in section 3.6 and 5 . [14]

3.5. Quark Fields

The quark contribution to the QCD action, S_{quark} called the *naive quark action*, is given by (18) where M is a $12 \times L^3T$ matrix, as the quark field is a 12-component field, D is a covariant derivative, and γ^μ are Dirac matrices.[14] [5]

$$S_{quark} = \sum_x \bar{\psi}(\gamma^\mu \cdot D_\mu + m)\psi = \bar{\psi}M\psi \tag{18}$$

M^{-1} is known as the quark propagator.[14] The naive quark action can be discretised to equation (19) using the finite difference Δ seen in (20).

$$S_{quark} = \sum_x \bar{\psi}(x)\left(\gamma \cdot \Delta + ma\right)\psi(x) \tag{19}$$

$$\Delta_\mu\psi(x) \equiv \frac{1}{2}\left(U_\mu(x)\psi(x + a\overrightarrow{\mu}) - U^\dagger_\mu(x - a\overrightarrow{\mu})\psi(x - a\overrightarrow{\mu})\right) \tag{20}$$

The gauge link U_μ arises as the covariant derivative is dependent on the gluon field $D_\mu = \partial_\mu - igA_\mu$. It can here be seen how gluon fields couple to the quarks which introduces more lattice parameters in form of the quark masses appearing in lattice units ma.[5]

In lattice QCD there is a distinct difference of how valence and sea quarks are handled. Valence quarks always have to be included as they contribute to the quantum numbers of hadrons. For sea quarks, only the light quarks u, d, s have a big influence on calculations and the heavier quarks c, b have little effect. The top quark t is never included, not even as a valence quark, due to its very short life-time. Both valence and sea quarks are represented in the matrix M seen in equation (18), respectively in M^{-1} and $\det(M)$. Different methods can be implemented in order to calculate these as described in sections 3.6 and 5. The determinant is very computationally heavy and therefore sea quarks are often left out, sometimes entirely which is called *quenched approximation* though this causes large systematic errors. Alternatively, most recent studies include the lighter quarks and some of the heavier quarks. The sea quarks are therefore often referred to as dynamical quarks. The number of sea quark included in a calculation is described using N_f where $N_f = 2$ is the inclusion of isospin light quarks $m_u = m_d$, $N_f = 2 + 1$ is the addition of the charm quark, and $N_f = 2 + 1 + 1$ includes the strange quark too. [14]

As the inclusion of quarks is computationally costly, the most common approach of handling them includes performing the calculations with unphysically large quark masses several times and then extrapolate to the physical masses. The masses of the u/d quarks are mostly given in terms of the mass of a pion meson m_π, having a physical mass of $m_\pi \approx 135MeV$, as it has quark combinations $u\bar{d}, u\bar{u}, d\bar{d}$ or $d\bar{u}$ depending on charge. [5]

Discretisation errors occour when including the heavy quarks (b and c) in lattice calculations as their masses, m_Q, are large and hence methods with errors related to ma will result in large errors. In particular if $m_Q a > 1$ then it is almost impossible to improve the method and get good results. An appropriate balance must be reached between the computational cost in choice of small a value and systematic errors. [14]

3.6. Methods

Lattice QCD calculations are very computationally heavy and the number of operations needed for a calculations is,

$$cost \approx \left(\frac{L}{a}\right)^4 \frac{1}{a}\frac{1}{m_\pi^2 a} \tag{21}$$

Hence it can be seen, that the choice of quark masses, lattice extent and especially lattice spacing is crucial for the cost of the calculations. But choosing small L, large a and m_π results in large discretisation errors and there is therefore a need for methods which can help reduce these errors.[13]

3.6.1. Discretising Gauge Action

For the gluonic contribution, the gauge action, to the continuum QCD action (16), the *Wilson action* is considered the simplest with the following discretisation,

$$S_W = \beta \sum_{x,\mu<\upsilon} (1 - P_{\mu\upsilon}(x)) \text{ with } \beta = \frac{6}{g^2} \tag{22}$$

Here $P_{\mu\upsilon}(x)$ is a 1×1 loop, the *plaguette*, as described earlier. This lattice discretisation sums over all possible plaquettes on the lattice with g the coupling constant being the only input parameter. The value of the latttice spacing a can only be determined after the calculations are done and it is dependent on g. Hence a is connected to the value of β where a larger value of β corresponds to a smaller a and therefore finer lattice. This method has discretisation errors of order $\mathcal{O}(a^2)$ [7] which corresponds to few percents difference when $\beta = 6.0 \rightarrow a = 0.1fm$ and hence in order to get more accurate results one needs to use a finer lattice spacing with much higher computational cost. Alternatively, an improved action was developed in order to decrease discretisation errors where the Wilson plaquette action is expanded in powers of a. [14] This was done through the addition of the 2×1 and 1×2 rectangle Wilson loops $\left(W_{\mu\upsilon}^{2\times1}, W_{\mu\upsilon}^{1\times2}\right)$ and resulted in the *Improved Wilson Action* (23). [21]

$$S_{W-improved} = \beta \sum_{x,\mu>\upsilon} \left(1 - \frac{5c_1}{3} P_{\mu\upsilon}(x) + \frac{c_2}{12}\left(W_{\mu\upsilon}^{2\times1}(x) + W_{\mu\upsilon}^{1\times2}(x)\right)\right) \tag{23}$$

Here c_1, c_2 are chosen such that the $\mathcal{O}(a^2)$ terms cancel out and hence resulting in errors of order $\mathcal{O}(a^4)$ only. Examples of this method are the *tree-level Lüsher Weisz action* (24) [21], the *classical (tree-level) lattice action* (25) [20], and the *Iwasaki action* (26). [7]

$$S_{LW} = \beta \sum_{x,\mu>\upsilon} \left(1 - \frac{1}{6}\left(\frac{3}{5}P_{\mu\upsilon}(x) - \frac{1}{12}W^{2\times1}_{\mu\upsilon}(x)\right) + h.c.\right) \tag{24}$$

Where $+h.c.$ means with hermitian conjugates.

$$S_{classical} = -\beta \sum_{x,\mu>\upsilon} \left(\frac{5}{3}P_{\mu\upsilon}(c) - \frac{1}{12}\left(R_{\mu\upsilon}(x) + R_{\upsilon\mu}(x)\right)\right) + const \tag{25}$$

Where $R_{\mu\upsilon}$ is the $2a \times a$ Wilson loop called the *rectangular operator*.

$$S_{Iwasaki} = \beta \sum_{\mu,\upsilon} \sum_{x} \left(P_{\mu\upsilon}(x) - 0.0907W^{1\times2}_{\mu\upsilon}(x)\right) \tag{26}$$

3.6.2. Discretising Fermion Action
When discretizing the quark fields an issue arises called the *fermion doubling problem*, which arises when the covariant derivative is symmetrically discretized. [5] It causes quark flavour multiplication and the naive quark action describes 16 quarks instead of just 1. [14] The Wilson action, as seen in equation (27) was proposed by Kenneth Wilson which adds a term to the naive action in order to give mass to the doublers. This is also known as *Wilson Fermions*.

$$S^{W}_{quark} = S^{naive}_{quark} - \frac{r}{2}\sum_{x} \bar{\psi}_x \Box \psi_x \tag{27}$$

$$\Box\psi_x = \sum_{\mu=1}^{4} U_\mu(x)\psi_{x+a\overrightarrow{\mu}} - 2\psi_x + U^{\dagger}_{\mu}(x - a\overrightarrow{\mu})\psi_{x-a\overrightarrow{\mu}}$$

Doing this, the doublers gets an increasingly large mass with decreasing lattice spacing effectively removing them in the continuum limit. This disadvantages of this method is discretisation errors of order $\mathcal{O}(a)$ causing large systematic errors. In order to improve the discretisation errors associated with the Wilson action, the *clover* action was introduced where a $\sigma_{\mu\upsilon}F^{\mu\upsilon}$ term cancels out with the $\mathcal{O}$ errors. The additional term discretises to setup that looks like a four-leaf clover consisting of a set of a plaquettes surrounding a central point.[14] Using Wilson fermions have a low computational cost but have some issues for example with chiral symmetry.[9]

Another method to handle fermion doubling is the unimproved staggered quark action, seen in equation (28). It is a converted (unimproved) naive quark action where quarks doesn't have spin. This is achieved through rotating the quark fields. Here $\mathcal{X}$ is a single-spin component field arising from $\psi \to \Omega(x)\mathcal{X}(x)$ and $\bar{\psi} \to \bar{\mathcal{X}}(x)\Omega^{\dagger}(x)$.

$$S^{S}_{f} = \sum_{x} \bar{\mathcal{X}}_x \left\{\frac{1}{2}\sum_{\mu} \alpha_{x,\mu}\left(U_\mu(x)\mathcal{X}_{x+a\overrightarrow{\mu}} - U^{\dagger}_{\mu}(x - a\overrightarrow{\mu})\mathcal{X}_{x-a\overrightarrow{\mu}}\right) + ma\mathcal{X}_x\right\} \tag{28}$$

This method does not solve the doubling problem but reduces it to be only 4 for every quark flavour instead of 16.[14] The staggered action has discretisation errors of order $\mathcal{O}(a)^2$ and it can be improved to reduce the discretisation errors even more.[9]

Sheikholeslami-Wholter (SW) proposed an addition to the Wilson action, a magnetic momentum term, in order to remove the $\mathcal{O}(a)$ errors but simultaneously keeping Wilson's solution for the fermion doubling problem. This resulted in the SW or clover action; [7]

$$S_{SW} = S_W - \frac{iaC_{SW}\kappa r}{4}\bar{\psi}(x)\sigma_{\mu\upsilon}F_{\mu\upsilon}\psi(x) \tag{29}$$

$\sigma_{\mu\upsilon}F^{\mu\upsilon}$ is a discretised set of plaquettes surrounding a point and hence looking like a four-leaf clover. σ is the 'string tension' [14], $\kappa = 1/(2m_q a + 8r)$ a rescaling factor [7] and C_{SW} a coefficient. C_{SW} takes different values depending on the method in use, for example for tree-level improvement $C_{SW} = 1$. The errors associated with this method are either $\mathcal{O}(a^2)$ classically or are reduced to $\mathcal{O}(\alpha_s a)$ where α_s is the strong coupling constant using quantum corrections. These quantum corrections can be calculated perturbatively or non-perturbatively. [21]

Fermilab developed a method for heavy quarks which relies on the Wilson action and uses both Wilson fermions and the clover action.[22] It works to remove $\mathcal{O}(a)$ errors whilst also handling ma errors in order to reliably simulate systems with charm and bottom quarks.[7]

A method called the *Wilson Twisted Mass QCD* adds a term (30), the *twisted mass* term, in order to have the standard quark mass be zero. This method gets rid of $\mathcal{O}(a)$ errors associated with the Wilson action.[23]

$$i\mu_q\bar{\mathcal{X}}\gamma_5\tau^3\mathcal{X} \tag{30}$$

Here τ^3 is a Pauli matrix and μ_q is the twisted mass. Using this, the standard Wilson twist mass action can be set up for light degenerate quarks up and down (31) and the Wilson twisted mass for non-degenerates heavy quarks charm and strange (sea quarks) (32).

$$S_{light}\left[\mathcal{X}^{(l)}, \bar{\mathcal{X}}^{(l)}, U\right] = \sum_x \bar{\mathcal{X}}^{(l)}(x)\left(D_w(m_0) + i\mu_q\gamma_5\tau^3\right)\mathcal{X}^{(l)}(x) \tag{31}$$

$$S_{heavy}\left[\mathcal{X}^{(h)}, \bar{\mathcal{X}}^{(h)}, U\right] = \sum_x \bar{\mathcal{X}}^{(h)}(x)\left(D_w(m_0) + i\mu_q\gamma_5\tau^1 + \mu_\delta\tau^3\right)\mathcal{X}^{(h)}(x) \tag{32}$$

Here D_w is the Wilson irac operator and $\mathcal{X}^{(l)} = \left(\mathcal{X}^{(u)}, \mathcal{X}^{(d)}\right)$, $\mathcal{X}^{(h)} = \left(\mathcal{X}^{(c)}, \mathcal{X}^{(s)}\right)$ are twisted basis quark fields.[24]

3.6.3. General Improvements

When expressing the gluon fields using exponentials a term appear which causes tadpole diagrams [7]; a Feynman diagram which is connected through only one line to the rest of the diagram. [25]These contribute to the correlation function and have associated errors, and hence in order to handle these every lattice operator is divided by the mean value u_0 of $\frac{1}{2}\mathrm{Re\ Tr}\, U_\mu(x)$. The mean value consist only of tadpoles and hence this cancels out all tadpoles, and this method is called *tadpole-improvement*. It is easily implemented in both gluon and quark actions through equation (34) [20]

$$U_\mu(x) \rightarrow \frac{U_\mu(x)}{u_0} \tag{33}$$

$$\alpha_{TI} = \frac{\alpha_l at}{u_0^4} \tag{34}$$

An example is the tadpole-improved improved Wilson action;

$$S_{W-improved} = \beta\sum_{x,\mu>\upsilon}\left(1 - \frac{5c_1}{3}\frac{P_{\mu\upsilon}(x)}{u_0^4} + \frac{c_2}{12}\frac{\left(W_{\mu\upsilon}^{2\times1} + W_{\mu\upsilon}^{1\times2}\right)}{u_0^6}\right) \tag{35}$$

Alternatively, the link operators in quark actions can be replaced by smeared links which consists a weighed average of the link and its neighbours.[26] The smeared gauge links leave the low-momentum components but they cut off the high-momentum components, resulting in reduced Monte Carlo statistical errors. [14] The simplest method of smearing is called *Gaussian* smearing, wheres as improvements to this method includes iterative smearing methods such as the Wuppertal smearing, and methods working to reduce noise in the Monte Carlo calculations such as APE and HYP smearing.[27] *APE (Array Processor Experiment)* smearing uses a relative strength α_{APE} to weight the neighbouring staples [3] added to the links. This process can be choosen to be iterated N_{APE} times. *HYP (Hyperbolic)* smearing consists of several steps using APE smearing and three weighting constants $\alpha_{HYP1}, \alpha_{HYP2}, \alpha_{HYP3}$.[28] Smearing can be implemented when creating operators and is used before applying the operator to the fields. An example, is the *distillation method* which, using smeared quark fields $\tilde{\Psi}$, defines meson creation operators

$$\mathcal{O}_M(t) = \overline{\tilde{\Psi}}(t)\Gamma\tilde{\Psi}(t) \tag{36}$$

Here Γ is a position, spin, colour space operator. [27] Distillation works in order to increase the overlap onto the state of interest and hence gives better results though it is very computationally costly. [29]

3.6.4. Lattice QCD Errors

Discretizing spacetime leads to systematic errors which are connected to the lattice spacing a where the smaller value will result in more accurate but also much more expensive calculations. [14] These errors are minimized through choice of method of latticec actions and operators, and through performing calculations using varying values of a and then extrapolating to $a = 0$. More errors arise when approximating derivatives on the lattice, the respective actions deal with these errors in different ways reducing them. Lattie QCD simplefies the infinite spacetime on to a finite lattice; when the lattice is small the wavefunctions of states will be squeezed and therefore their mass will be affected. The masses of up and down quarks are too light to perform calculations with as the computational cost is too high, therefore, like the lattice spacing, several simulations are done using varying masses and then extrapolated to the isospin symmetric mass $\bar{m} = (m_u + m_d)/2$. Breaking of isospin is believed to have little error associated with it and is often ignored together with contributions from electromagnetism.[7] Systematic errors arise from the Monte Carlo method which are decrease with the number of configurations used.[13] When extrapolating to continuum values, such as $a = 0$ and physical quarks masses, systematic errors arise.[15]

4. Experimental Results

4.1. $D_{s0}(2317)^{\pm}$

The particle was first experimentally observed decaying into $D_s^+\,\pi^0$ in positron-electron annihilation by the BARBAR Collaboration in April 2003.[30] Later the same year, both the Belle collaboration and CLEO collaborations observed it in $e^+\,e^-$ annihilations [31] [32], and the Belle collaboration in B meson decays.[33] The observed masses can be found in table 1 or a graphical depiction can be found on figure 3.

Results from particle collision are indirect measurements of the $D_{s0}(2317)$ meaning that the particle itself is not detected but its decay products are.[1] At the beginning, the particle was thought to be an excitation of a $c\bar{s}$ meson but the mass observed is around 160 MeV below expected and lies below the DK threshold (the needed mass for the particle to be able to decay into a D-meson and a K-meson).[2]

[3] Staples are paths with $U_v(x)U_\mu(x + a\overrightarrow{(}v)U_v(x + a\overrightarrow{\mu})$.[14]

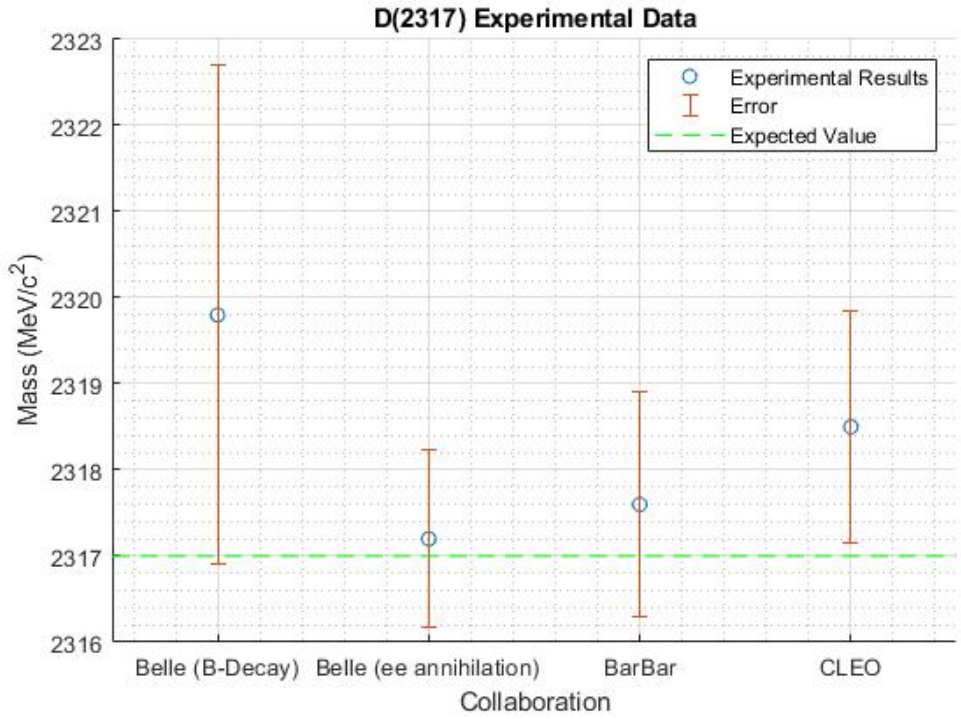

Figure 3: Graph of experimental results for $D_{s0}(2317)^{\pm}$ from [33], [32], [30] & [31]

	BARBAR	**Belle (e^+e^- annihilation)**	**CLEO**	**Belle (B-decay)**
Mass (MeV/c^2)	2317.6 ± 1.3	$2317.2 \pm 0.5 \pm 0.9$	2318.5 ± 1.34	$2319.8 \pm 2.1 \pm 2.0$

Table 1: Experimental results for $D_{s0}(2317)^{\pm}$ from [30], [31], [32], & [33].

The BARBAR collaboration did not find any sign of the particle decaying into any other of the predicted particle combinations and the models at the time were therefore questioned.[30] Because of these things, it has been proposed that the D_{s0} is an exotic meson which could have the structure of a meson-meson molecule, a tetraquark or other configurations.[34] A meson-meson molecule consists of two mesons bound together by hadronic interactions, where the quark and antiquark in each meson are bound together more strongly than the two mesons are bound with each other. On the contrary, in a tetraquark all quarks are equally bound to each other.[35] The structures are most often thought to consist of two heavy quarks and two light quarks which are depicted as $Q, \bar{Q}$ for the heavy and $q, \bar{q}$ for the light on figure 4. It is currently not possible to experimentally differentiate the two different structures.[1] The quark content of the D_{s0} as a tetraquark is unknown but must contain at least a charm and anti-strange.[2]

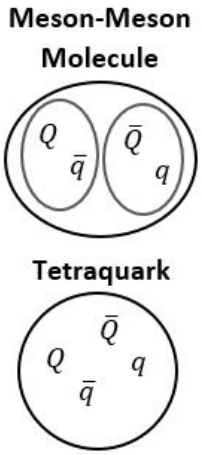

Figure 4: Depiction of meson-meson molecule and tetraquark structures.

4.2. $Z_c^{\pm}(3900)$

The particle was first observed in $e^+e^- \to \pi^+\pi^- J/\Psi$ processes by the BESIII Collaboration in 2013 [36]. It was later the same year confirmed by the Belle collaboration [37] and by researches going through data from the CLEO-c detector at CESR [38]. The observed masses can be found in table 2 or a graphical depiction can be found on figure 5. These results were exciting as the Z_c was observed decaying into charged pion $\pi^{\pm}$ and a J/Ψ-meson, $\pi^+ : u\bar{d}$, $\pi^- : \bar{u}d$, $J/\Psi : c\bar{c}$. Due to the large mass of the Z_c, it will most likely contain a charm and an anticharm, but it has total charge of ± 1 and hence it must contain two more quark making it a strong tetraquark candidate.[39] It has, like the $D_{s0}(2317)^{\pm}$, also been proposed to be a meson-meson molecule.

	BESIII	**Belle**	**CLEO**
Mass $(\mathbf{MeV/c^2})$	$3899.0 \pm 3.6 \pm 4.9$	$3894.5 \pm 6.6 \pm 4.5$	$3886 \pm 4.0 \pm 2.0$

Table 2: Experimental Results for $Z_c^{\pm}(3900)$ from [36], [37], and [38].

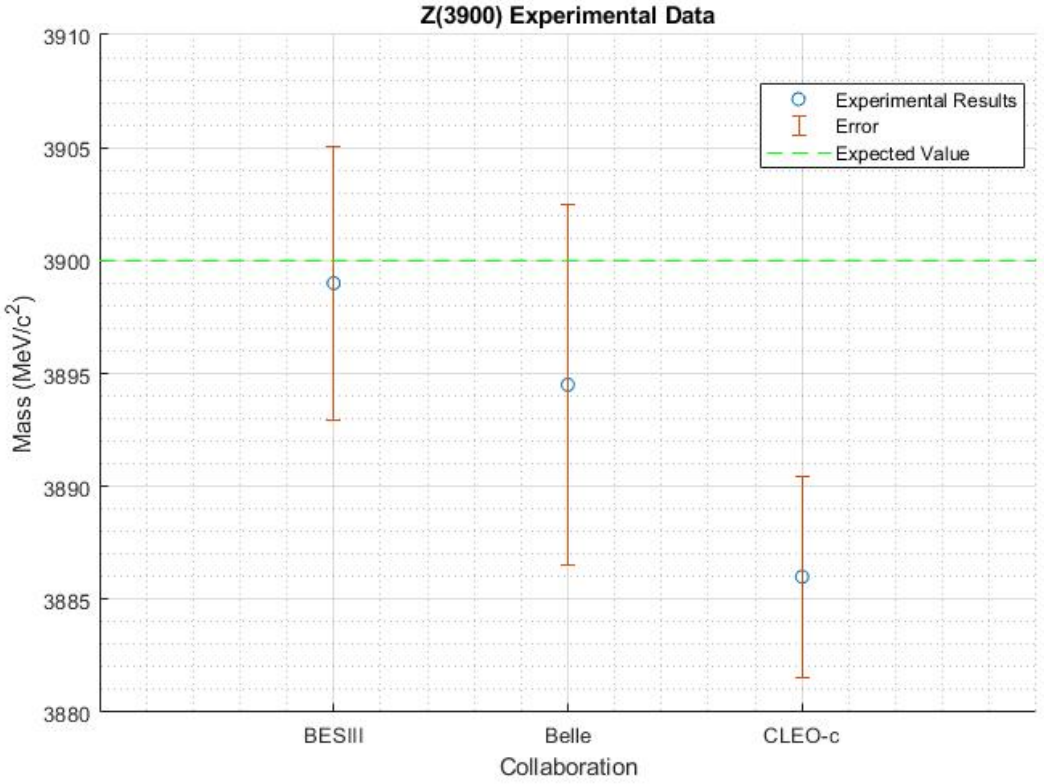

Figure 5: Graph of experimental results for $Z_c^{\pm}(3900)$ from [36], [37], and [38].

5. Lattice QCD Results

5.1. $D_{s0}(2317)^{\pm}$

Several lattice QCD studies has focused on the $D_{s0}(2317)^{\pm}$; the first studies used the quenched approximation [40], only using quark-anitquark interpolation operators and did therefore substantially overestimate the mass. [34] In this review results from three separate studies are presented, all studies observed an energy level which corresponded to the D_{s0} and their results can be seen in table 3 or on figure 6.

	RQCD	**Twisted Mass**	**Mohler *et al.* (1)**	**Mohler *et al.* (2)**
Mass ($\mathbf{MeV/c^2}$)	$2348 \pm 4 \pm 6$	2390 ± 25	$2363.2 \pm 5 \pm 3$	$2342 \pm 16 \pm 4$

Table 3: Lattice QCD Results of D^*_{s0} from [34], [24], & [40]

All results are at least $25\,\mathrm{MeV/c^2}$ above the expected value of $2317\,\mathrm{MeV/c^2}$ which could be a result of systematic errors connected to lattice QCD or the individual choices of lattice setup. Both the RQCD collaboration and the Twisted Mass researchers [4] performed lattice simulations using ensembles of varying lattice parameter and the result stated in table 3 are their final result. Mohler *et al.* used only two ensembles and therefore both their results are stated. A comparison of methods can be found in 6.1.

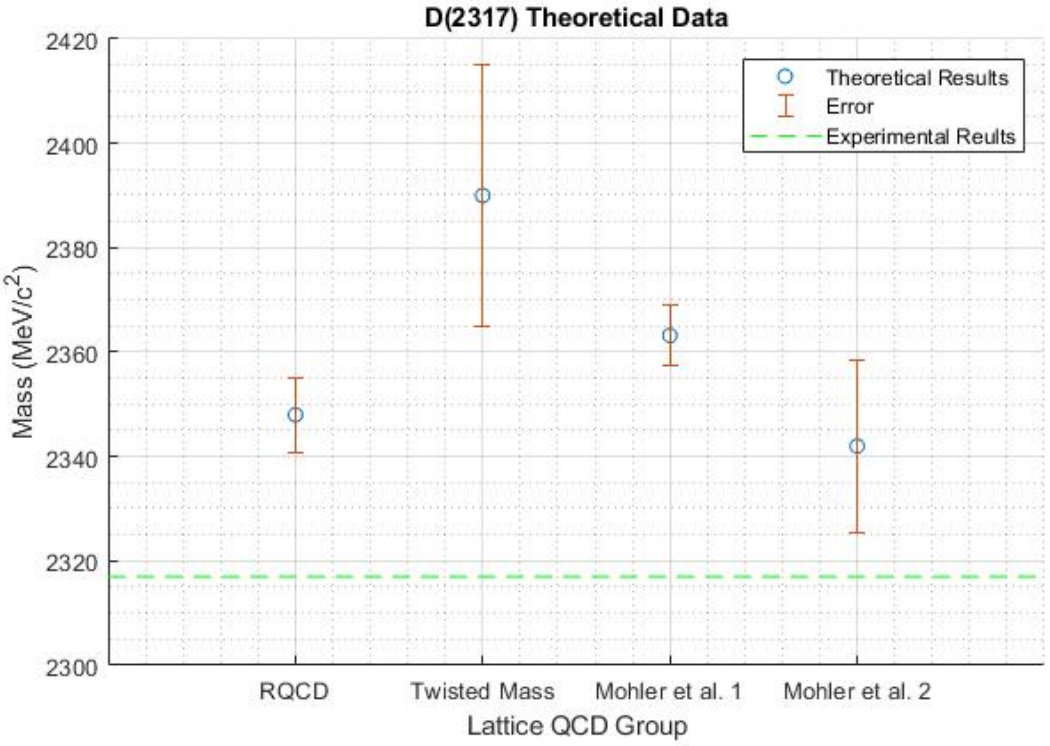

Figure 6: Graph of lattice QCD results for $D_{s0}(2317)^{\pm}$

[4] The name Twisted Mass was chosen as this group of researches used a method called Twisted Mass to setup their lattice calculations.

5.2. $Z_c^{\pm}(3900)$

In this review two studies ([16] and [17]) are included for the lattice QCD results for the Z_c, the resultant energy levels can be seen in figure 7. Here the energy levels are depicted as coloured boxes for 7a and as black spheres for 7b. On the right of both plots, the horizontal lines represent expected energy levels for meson-meson states. Both studies show results from using different part of their operator sets; using all operators and using only either meson-meson or 4-quark operators. Comparing the results, one can see that excluding the 4-quark operators does not have a particularly strong effect. On 7a, one can see that the energy levels found using only 4-quark operators are poorly determined as "a reliable spectrum could not be extracted". [16] Observing the energy levels, all are found to correspond to a meson-meson state, and an additional energy level, which would correspond to the Z_c, is not found. This could be because the studies were not precise enough to render the energy level and that for example, one of the energy levels is actually two close energy levels with the calculations not precise enough to distinguish them. The possible reasons for this are discussed later in 6.1.[34] The Z_c has only been observed in $e^+e^- \rightarrow Y(4260) \rightarrow (J/\Psi\pi^+)\pi^-$, but not in other expected decay schemes, at least not yet, which hints towards the indication that the experimental results could have a different origin. [17] An alternative suggestion is that the observations are a result of an interaction between two D mesons [39].

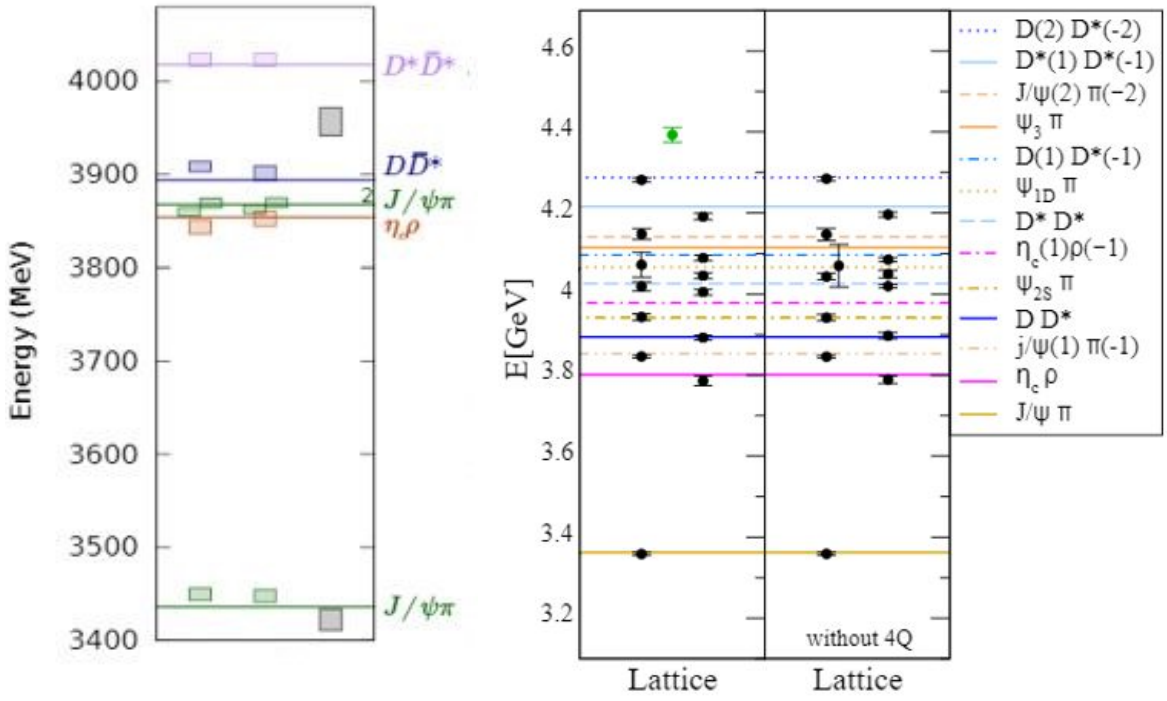

(a) Energy level results from [16]

(b) Energy level results from [17]

Figure 7: Lattice QCD results from studies looking for $Z_c^{\pm}(3900)$. For 7a, the first column all operators used and the second column only meson-meons operators. For 7b the first Column all operators used, second column only meson-meson operators, and third column only 4-quark operators.

6. Discussion

6.1. Comparison of Lattice QCD Studies:

6.1.1. $D_{s0}(2317)^{\pm}$

The studies used different lattice parameters and methods for setting up the calculations which influenced their overall result and the associated errors. The choices of lattice parameters can be seen in table 4, where several studies had an interval of values for one ensemble. For example, in the first ensemble from RQCD several different lattice volumes from $24^3 \times 48$ to $64^3 \times 64$. Parameters in square brackets represents intervals of values whilst vertically aligned values in a cell represent two different values used.

	a (fm)	**L (fm)**	$\mathbf{m_\pi}$**(MeV)**	$\mathbf{N_f}$	**Volume**	**# configs**
RQCD (1)	0.071	[1.7,4.5]	290	2	$[24^3\times48, 64^3\times64]$	[1453,2222]
RQCD (2)	0.071	[3.4,4.5]	150	2	$48^3 \times 64$ $64^3 \times 64$	1591 2501
Twisted Mass	0.0619 0.0885	[2.124,2.971]	[225,470]	2+1+1	$[24^3\times48, 48^3\times96]$	[132,11176]
Mohler *et al.* (1)	0.1239	1.98	266	2	$16^3 \times 32$	279
Mohler *et al.* (2)	0.0907	2.9	156	2+1	$32^3 \times 64$	196

Table 4: Comparison of Lattice Parameters for Lattice QCD Studies of D^*_{s0} from [34], [24], & [40]

The lattice spacing, a, choosen affects the error on the result; the smaller the value the more precise the result though at a higher computational cost. Comparing the lattice spacing from the separate studies, the RQCD and the Twisted Mass use similar and relatively small values for a whilst Mohler *et al.* have higher values (especially for their first ensemble). This would have cost them greater systematic errors, but these could be canceled out depending on their choices of other lattice parameters and methods. A certain spatial extent, L, is needed in order to render specific energy levels, as for example the size of the hadron must fit comfortably in the spatial extent.[5] All studies used similar spatial extents, except for the second set of ensembles from RQCD using $m_\pi = 150MeV$ which use much larger values. The value for the up and down quark are directly connected to the mass of the pion (m_π), hence a large value of (m_π) means unphysically heavy u/d quarks. The physical mass is $\approx 135MeV$ and hence all studies used heavy u/d quarks, where only the second ensembles from RQCD and Mohler *et al.* used close to physical values. Though the Mohler study compensated for the higher computational cost by using a smaller set of configurations. The number of sea quarks included in the study has an affect on the overall result and error of the calculations; including more sea quark flavours give more precise results but is much more computationally heavy. Only the Twisted Mass study includes all quarks as sea quarks, where RQCD and Mohler uses only u/d quarks (and charm quarks for the second ensembles from Mohler). Looking at the results on figure 6, this is counter-intuitive as the Twisted Mass study have the most inaccurate results both with respect to both overall result and errors. Comparing the two ensembles from Mohler, it can seen that the second ensemble has a result much closer to the actual value which shows that using more physically accurate quark masses, $N_f = 2 + 1$ and larger volume will give better results.

The lattice volume can alter the overall result, as a too small volume can result in energy levels not being rendered. This is due to for example, the lattice volume being too small to distinguish structures.[16] The volume states in table 4 are structured as $\mathrm{L/a}^3 \times$temporal extent. All studies use between 24^3 and 48^3 for L/a^3, with the exception of the first ensemble from Mohler. The number of configurations used describes the number of paths and hence interpolating operators used which, if a small number of operators used, could mean that energy levels do not show up.[34] The Mohler study uses much fewer configurations, though looking at their results, this did not seem to have a big influence. The Twisted Mass study was much more thorough than the two others which can be seen in the table as a range of values was used for each lattice parameter. They studies masses of D, D_s mesons and charmonium states whereas the other studies only focused on $D_{s0}(2317)^{\pm}$. This meant that their basis of interpolating functions must have been much more general which could have affected their result.

Table 5 show a simple overview of the methods used by each study. All energy levels from the studies were extracted using the variational method; the generalized eigenvalue problem, and hence this was not included in the table.

	RQCD	**Twisted Mass**	**Mohler *et al.***
Ensembles	Improved Clover action	Iwasaki action	Improved Wilson Action
Heavy-Quark Discretization	Partially quenched	Wilson Twisted Mass	Fermilab Method
Quark field Smearing	Wuppertal smearing w. APE links	APE smearing & Gaussian smearing	Laplacian-Heaviside smearing & Stochastic extended smearing
Correlation Function	Stochastic one-end trick	Stochastic one-end trick	Distillation Method

Table 5: Comparison of Methods for Lattice QCD Studies of D^*_{s0} from [34], [24], & [40]

All studies used a form of improved Wilson action and therefore have systematic errors connected with the discretisations of spacetime of less than or equal to order $\mathcal{O}(a^2)$. Monte Carlo integration is used in all calculations and in order to improve computational efforts, the Hybrid Monte Carlo method can be used. It reduces the computational cost and therefore values for lattice spacing, lattice extent and quark masses given more accurate results can be chosen.[9] Mohler *et al.* used slightly different methods when it came to their smearing and distillation, which resulted in the big difference in errors seen on the figure. The Twisted Mass study used only meson-meson operators whereas the other studies also used 4-quark operators. This could have caused their result to be much further from the experimental value than the other results. They also present a much more thorough error-analysis than the other studies, this could be the reason for why they have much larger errors. This could also be a result of their choice of using Twisted mass methods.

6.1.2. $Z_c^{\pm}(3900)$

The lattice parameters for the two studies are shown in table 6.

	a (fm)	**L (fm)**	$\mathbf{m_\pi(MeV)}$	$\mathbf{N_f}$	**Volume**	**# configs**
Prelovsek *et al.*	0.1239	1.98	266	2	$16^3 \times 32$	280
Cheung *et al.*	0.12	2	391	2+1	$16^3 \times 128$	478

Table 6: Comparison of Lattice Parameters for Lattice QCD Studies of Z_c by [17] and [16]

It can here be seen that the studies use almost the same values for the lattice spacing a and the spatial extent L. The lattice spacing is, compared with the studies related to the $D_{s0}(2317)^{\pm}$, quite large which results in rather large systematic errors. The spatial extent is quit small, and the quark masses are unphysically large. Both of these two factors, small L and large m_π could have resulted in the absence of the Z_c-energy level. The fact that the mass of the up and down quarks are set to be equal could also have had a great influence on the results. Both studies have a rather small number of configurations and there may not have been enough to render the energy level. [17] [16] Neither study include all sea quarks which again introduces errors and both studies performed calculations with just one lattice spacing and therefore did not extrapolate to $a = 0$, though this is not believed to have had a crucial influence on the results. It is not expected that this is the reason for the absent energy level.[17] Generally, both studies performed calculations on only one ensemble and hence in order improve the results more ensembles needs to included in order to study the dependence on light quark masses, lattice extent, etc. [16]

	Prelovsekc *et al.*	**Hadron Spectrum**
Ensembles	Tree-level Improved Wilson-Clover Action	Tree-level Symanzik Improved Gauge Action & Clover Fermion Action
Heavy-Quark Discretization	Fermilab Method	Quenched Clover Charm Quark
Quark field Smearing	Laplacian Heaviside Smearing	Distillation Operator
Correlation Function	Distillation Method	Distillation Method

Table 7: Comparison of Methods for Lattice QCD Studies of D_{s0}^* from [34], [24], & [40]

The two studies used different methods to setup their lattice calculations which can be seen in a basic overview in table 7. Both studies use a type of Improved Wilson Action when discretising the gauge and fermion action, they implement smearing and discretisation in order to minimize errors. The distillation method was used by both studies when setting up the correlation functions, and the variational method was used in order to extract energy levels. There can therefore not be drawn any conclusions to the absence of a Z_c energy level from the choices of methods.

6.2. ***Future of Tetraquarks:***
The two cases presented here have very different results; the $D_{s0}(2317)^{\pm}$ has been observed in several decay schemes and have been confirmed by lattice QCD. But there is a good chance that this is "just" an excited state of a $c\bar{s}$ meson. The $Z_c^{\pm}(3900)$ has only been observed in one specific decay and has been absent in others where it has been excepted to be seen.[1] It has not been confirmed by lattice QCD studies yet which, as previously mentioned, could point to an inaccuracy in the lattice QCD studies or to a different origin for the experimental results. It is an option that all exotic hadrons observed so far are not as exciting as many hope them to be, but that they are effects of kinematics of decays. If this was to be the case it would still point to a lack of understanding of the dynamics of QCD. [2]

There is also the possibility that these particles are meson-meson molecules, which would open the door for many other particles with similar structures. The theory of the exotic hadrons being meson-meson molecules include the states having matching quantum numbers and masses close to the threshold of a regular meson decaying into the two mesons involved in the molecule. It is possible that some of the states are tetraquarks whereas others are meson-meson molecules and/or decay kinematics. If a tetraquark were to be confirmed by an agreement between both experimental and theoretical results it follows that many tetraquark states have yet to be observed. [1].

In the future, experiments at LHC and Belle are hoping to gain more information on the already found states and potentially new states. This includes looking for expected decay modes for the exotic hadrons and searching for new particles which could either determine the exact structure or rule out options. [1]

7. Conclusion
Several exotic hadrons have been exprimentally observed with properties (quantum numbers, decay schemes, masses) which do not match with the quark model. So far there has not been any definite conclusion drawn about the structures of these particles, as they could be tetraquark, meson-meson molecules, or effects of decay kinematics. This review presented the experimental results and some lattice QCD studies for the two exotic states $D_{s0}(2317)^{\pm}$ and $Z_c^{\pm}(3900)$. For the D_{s0} the experimental and theoretical results agree within an acceptable margin. For $Z_c^{\pm}(3900)$ the experimental results agreed with each other and suggest it being an exotic meson, but the lattice QCD studies did not find it. Therefore no overall conclusion can be drawn; Tetraquarks could exist, though theoretical and experimental results must agree in order to finally decide

References

[1] Cowan, G. & Gershon, T., *Tetraquarks and Pentaquarks*, IOP Publishing, 2018, 1-24
[2] Swanson, E. S., *The New heavy mesons: A Status report.*, Phys. Rept. **429** (2006) 243, 12-17 & 44-54
[3] HyperPhysics, *Gluons*, Available at : `http://hyperphysics.phy-astr.gsu.edu/hbase/Particles/expar.html`, [Accessed December 14. 2018]
[4] HyperPhysics, *Quarks*, Available at : `http://hyperphysics.phy-astr.gsu.edu/hbase/Particles/quark.html`, [Accessed December 14. 2018]
[5] Wagner, M., Diehl, S., Kuske, T., and Weber, J., *An introduction to lattice hadron spectroscopy for students without quantum field theoretical background*, 2013, 1-27
[6] Davies, C. *Colourful Calculations*, Physics World December 2006
[7] Gupta, R., *Introduction to lattice QCD: Course*, Los Alamos National Laboratory, 1997, 1-100
[8] Klempt, E. and Zaitsev, A., *Glueballs, Hybrids, Multiquarks. Experimental facts versus QCD inspired concepts.*, Phys. Rept. **454** (2007) 1, 1-28
[9] Hashimoto, S., Laiho, J. and Sharpe, S. R., *Lattice Quam Chromodynamics*, Peview of Particle Properties, 2017, 1-27
[10] Encyclopædia Britannica, *Parity* [ONLINE], Available at:`https://www.britannica.com/science/parity-particle-physics`, [Accessed December 3. 2018]
[11] Encyclopædia Britannica, *Charge Conjugation* [ONLINE], Available at:`https://www.britannica.com/science/charge-conjugation`, [Accessed December 17. 2018]

[12] Miller, D. J., *PHYS 4026 Quantum Theory Course Notes*, University of Glasgow School of Physics & Astronomy, 2018, 14-16
[13] Lepage, G. P. *Lattice QCD for novices*, Strong interactions at low and intermediate energies. Proceedings, 13th Annual Hampton University Graduate Studies, HUGS'98, Newport News, USA, 1998, 49-90
[14] Davies, C., *Lattice QCD: A Guide for people who want results.*, Lectures at 58th Scottish Universities Summer School in Physics, 2004, 1-20
[15] Ukawa, A., *Kenneth Wilson and lattice QCD.*, J. Statist. Phys. **160** (2015) 1081, 26-29
[16] Cheung, G. K. C., *et al.* [Hadron Spectrum Collaboration], *Tetraquark operators in lattice QCD and exotic flavour states in the charm sector*, JHEP **1711** (2017) 033, 1- 31
[17] Prelovsek, S., Lang, C. B., Leskovec, L., and Mohler, D., *Study of the Z_c^+ channel using lattice QCD*, Phys. Rev. D **91** (2015) no.1, 014504, 1-11
[18] WriteOpinions, *Opinions on Lattice QCD* [ONLINE], Available at: `http://www.writeopinions.com/lattice-qcd`, [Accessed December 12. 2018]
[19] Bhalerao, R. S. and Gavai, R. V., *Heavy Ions at LHC: A Quest for Quark-Gluon Plasma*, Physics at the Large Hadron Collider, 2008, 3
[20] Lepage, G. P., *Redesigning lattice QCD*, Lect. Notes Phys. **479** (1997) 1, 1-25
[21] Hoelbling, C., *Lattice QCD: concepts, techniques and some results*, Acta Phys. Polon. B **45** (2014) no.12, 2143, 1-20
[22] Oktay, M. B. and Kronfeld, A. S., *New lattice action for heavy quarks*, Phys. Rev. D **78** (2008) 014504, 1-13
[23] Shindler, A., *Twisted mass lattice QCD*, Phys. Rept. **461** (2008) 37, 1-15
[24] Cichy, K., Kalinowski, M., and Wagner, M., *Continuum limit of the D meson, D_s meson, and charmonium spectrum from $N_f = 2 + 1 + 1$ twisted mass lattice QCD*, Phys. Rev. D **94** (2016) 094503, 1-29
[25] Evans, T., *'Diagramology', Types of Feynman Diagram*, Imperial College of Science, 2018, 1-2
[26] Solbrig, S. *et al.*, *Smearing and filtering methods in lattice QCD: A Quantitative comparison*, PoS LATTICE **2007** (2007) 334, 1-3
[27] Ryan, S. M., *Lattice Methods for Hadron Spectroscopy*, Lattice QCD for Nuclear Physics, Chapter 2, 2015, 1-50
[28] Alexandrou, C. *et al.*, *Comparison of topological charge definitions in Lattice QCD*, DESY 17-115, 2017, 1-18
[29] Peardon, M. *et al.* [Hadron Spectrum Collaboration], *A Novel quark-field creation operator construction for hadronic physics in lattice QCD*, Phys. Rev. D **80** (2009) 054506, 1-10
[30] Aubert, B. *et al.* [BaBar Collaboration], *Observation of a narrow meson decaying to $D_s^+\pi^0$ at a mass of 2.32 GeV/c^2*, Phys. Rev. Lett. **90** (2003) 242001, 1-7
[31] Besson, D. *et al.* [CLEO Collaboration], *Observation of a narrow resonance of mass 2.46-GeV/c**2 decaying to D*+(s) pi0 and confirmation of the D*(sJ)(2317) state*, Phys. Rev. D **68** (2003) 032002, 1-10
[32] Mikami, Y. *et al.* [Belle Collaboration], *Measurements of the D_{sJ} resonance properties*, Phys. Rev. Lett. **92** (2004) 012002, 1-5
[33] Krokovny, P. *et al.* [Belle Collaboration], *Observation of the $D_{sJ}(2317)$ and $D_{sJ}(2457)$ in B Decay*, Phys. Rev. Lett. **91** (2003) 262002, 1-6
[34] Bali, G. S., Collins, S., Cox, A. and Schäfer, A. [RQCD Collaboration], *Masses and decay constants of the $D_{s0}^*(2317)$ and $D_{s1}(2460)$ from $N_f = 2$ lattice QCD close to the physical point*, Phys. Rev. D **96** (2017) no.7, 074501, 1-24
[35] Braaten, E., Langmack, C., and Smith, D. H., *Born-Oppenheimer Approximation for the XYZ Mesons.*, Phys. Rev. D **90** (2014) no.1, 014044, 1-2
[36] Ablikim, M. *et al.* [BESIII Collaboration], *Observation of a Charged Charmoniumlike Structure in $e^+e^- \to \pi^+\pi^- J\Psi$ at $\sqrt{s} = 4.26 GeV$.*, Phys. Rev. Lett. **110** (2013) 252001, 1-7
[37] Liu, Z. Q. *et al.* [Belle Collaboration], *Study of $e^+e^- \to \pi^+\pi^- J/\Psi$ and Observation of a Charged Charmoniumlike State at Belle.*, Phys. Rev. Lett. **110** (2013) 252002, 1-10
[38] Xiao, T., Dobbs, S., Tomaradze, A. and Seth, K. K., *Observation of the Charged Hadron $Z_c^{\pm}(3900)$ and Evidence for the Neutral $Z_c^0(3900)$ in $e^+e^- \to \pi\pi J/\Psi$ at $\sqrt{s} = 4170$ MeV.*, Phys. Lett. B **727** (2013) 366, 1-6
[39] Swanson, E., *New Particle Hints at Four-Quark Matter*, Physics **6**, 69 (2013), 1-3
[40] Mohler,D., Lang, C. B., Leskovec, L., Prelovsek, S., and Woloshyn, R. M., *$D_{s0}^*(2317)$ meson and D-meson-kaon scattering from lattice QCD*, Phys. Rev. Lett. **111** (2013) 222001, 1-5